In-Vivo NIRS and Muscle Oxidative Metabolism

5

Takafumi Hamaoka

5.1 Introduction

Muscle oxidative metabolism has often in the past been examined by traditional analytical biochemistry based on obtaining biopsy samples. Invasive techniques such as intravascular catheterization have provided information on muscle oxygen status at rest and during exercise [1]. Myoglobin O_2 saturation and reduced nicotinamide adenine dinucleotide (NADH) redox state can be detected using freeze-clamped tissue [2]. The disadvantages of the invasive approach include poor time resolution due to repeated measurements and, of course, the invasive nature of the sampling method, so there is a need for noninvasive approaches to measure muscle oxygen status during exercise. NIRS has been utilized to evaluate skeletal muscle O_2 dynamics and energetics during exercise. Application of this technology has focused on the validity and calibration of measurements, and biochemical, physiological, and pathological research of muscle oxidative metabolism [3–6]. The primary reason why NIRS methodology is useful for evaluating muscle is the visibility of heme molecules and their oxygen-dependent characteristics.

Visible light has been used to monitor changes in tissue oxygenation since the 1930s [7]. Mitochondrial NADH signal measured using optical methods has shown a rapid change caused by electrical muscle stimulation (within a fraction of a second), indicating coupling of muscle contraction and mitochondrial activity [8, 9]. Jöbsis [10] then discovered that NIR light easily penetrates the skull, which set the stage for recent application of NIRS to scientific research in brain and muscle as well as in various clinical settings. A muscle NIRS system was then developed [11–13] that served as one of the first models to provide an opportunity for noninvasive and portable clinical muscle research.

5.2 Biochemistry and Physiology of Muscle Oxidative Metabolism

Skeletal muscle employs three major biochemical processes to synthesize ATP: oxidative phosphorylation (32–36 ATPs), anaerobic glycolysis (2 ATPs), and the PCr pathway (1 ATP). During low- to moderate-intensity exercise, like that involved in normal daily activities, skeletal muscle intensively

T. Hamaoka, M.D., Ph.D. (✉)
Department of Sport and Health Science, Ritsumeikan University, 1 Nojihigashi, Kusatsu, Shiga, Japan
e-mail: kyp02504@nifty.com

T. Jue and K. Masuda (eds.), *Application of Near Infrared Spectroscopy in Biomedicine*, Handbook of Modern Biophysics 4, DOI 10.1007/978-1-4614-6252-1_5,

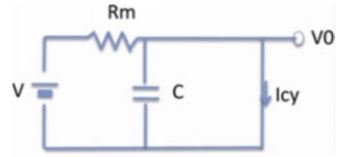

Fig. 5.1 Electrical analog model with a first-order linear system for respiratory control in muscle at submaximal oxidative rates. The current Icy represents the cytosolic adenosinetriphosphatase (ATPase) rate, the voltage V0 represents the free energy potential available in the mitochondria. Capacitance C is due to the creatine kinase reaction, and PCr is analogous to stored charge on a capacitor. Resistor Rm is a function of the number and properties of the mitochondria in the cell, and current Irm is the rate of oxidative phosphorylation [18]

relies on oxidative metabolism. Skeletal muscle O_2 consumption (VO_2) can be elevated 50-fold with up to tenfold abrupt increases in O_2 delivery (DO_2). The net oxidative energy pathway in muscles can be described by the following equation [14]:

$$3\text{ADP} + 3\text{Pi} + \text{NADH} + \text{H}^+ + {}^1\!/_2\text{O}_2 = 3\text{ATP} + \text{NAD}^+ + \text{H}_2\text{O}, \tag{5.1}$$

where ADP is adenosine diphosphate, Pi is inorganic phosphate, ATP is adenosine triphosphate, and NAD^+ is the nicotinamide adenine dinucleotide.

The kinetic control model of respiration that describes metabolic rate as a function of regulatory substrate concentrations using the Michaelis-Menten equation is written as [15]

$$V/V_\text{m} = 1/(1 + k_1/\text{ADP} + k_2/\text{Pi} + k_3/\text{O}_2 + k_4/\text{NADH}), \tag{5.2}$$

where V is observed velocity, V_m is maximum velocity, k_{1-4} represent affinity constants for various substrates, Pi is inorganic phosphate, PCr is phosphocreatine, and NAD is the nicotinamide adenine dinucleotide. The in-vivo mitochondrial concentrations of ADP, Pi, O_2, and NADH are around 20, 1,000, 1, and 100 μM, respectively, and the in-vitro K_m (half-maximum velocity) values for ADP, Pi, O_2 (cytochrome aa3 for O_2), and NADH are 20, 300, 0.1, and ~10 μM, respectively. The in-vitro data indicate that the primary candidate for metabolic control is ADP [15]. However, it should be noted that no final agreement has been reached as to what is the metabolite controller of mitochondrial respiration.

For the phosphorylation cycle to function, ADP and Pi must be transported into the mitochondrial matrix, and then ATP is transported from there back to the cytoplasm. This reaction is catalyzed by the adenine nucleotide translocase of the inner mitochondrial membrane. It has thus been proposed that the rate of mitochondrial respiration can be determined by the rate of adenine nucleotide translocation and that, therefore, the [ATP]/[ADP] ratio regulates the respiratory rate under physiological conditions [16]. Holian et al. [17] generalized metabolic regulation to include ATP as a controller, as well as ADP and inorganic phosphate. The near-equilibrium hypothesis states that there is a correlation among the cellular [ATP]/[ADP][Pi] ratio, the mitochondrial [NAD]/[NADH] ratio, and respiration rate. Respiration rate would thus be dependent on [ATP]/[ADP][Pi] under conditions of Pi (~1 mM) and ATP (~6 mM). In general, ATP is maintained constant during submaximal exercise by creatine kinase equilibrium via the creatine shuttle in muscle, and ATP is not operative in respiration regulation.

The thermodynamic regulation model [18], an analogue of the electrical model for respiration control, in which PCr can be directly related to respiration rate, should thus be applicable to mitochondrial respiration (see Fig. 5.1). The current (I_cy) represents the cytosolic adenosine triphosphatase (ATPase) rate, and voltage V_0 represents the free energy potential available in the mitochondria. Capacitance C is due to the creatine kinase reaction, and PCr is analogous to the stored

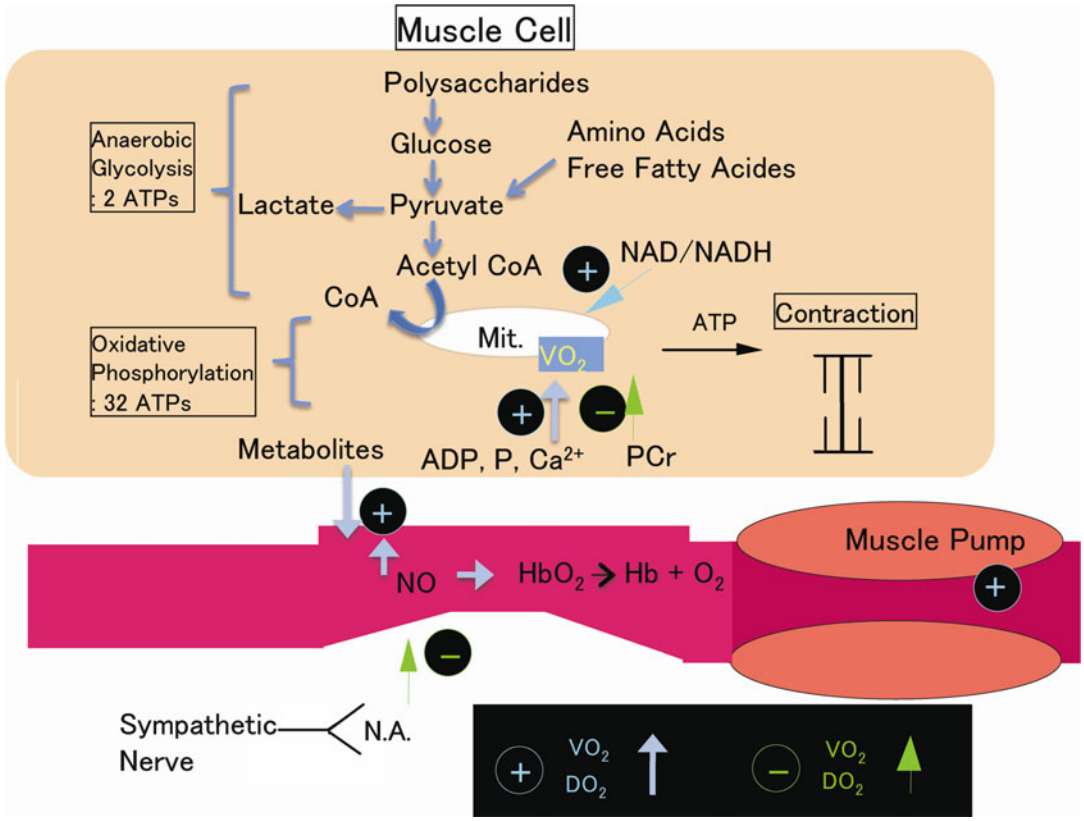

Fig. 5.2 Cellular mechanism for mitochondrial respiration and oxygen delivery to muscle. Mitochondrial respiration is controlled by the concentrations of ADP, Pi, and Ca^{2+}, the NAD/NADH ratio, and so on. Oxygen delivery (blood flow) is controlled by sympathetic vasoconstriction, varying metabolites, NO, muscle pump, etc. ATP is synthesized via the three main steps – namely, oxidative phosphorylation (32 ATPs), anaerobic glycolysis (2 ATPs), and PCr pathway (1 ATP). *Mit* mitochondrion, *NA* noradrenaline, *NO* nitric oxide: HbO_2 oxyhemoglobin, *ATP* adenosine triphosphate, *ADP* adenosine diphosphate, *Pi* inorganic phosphate, *PCr* Phosphocreatine, *NAD* nicotinamide adenine dinucleotide, *NADH* reduced nicotinamide adenine dinucleotide, VO_2 oxygen consumption: DO_2, oxygen delivery

charge on a capacitor. Resistor R_m is a function of the number and properties of the mitochondria in the cell, and current I_{rm} is the rate of oxidative phosphorylation [18], where $I_{rm} = I_c + I_{cy}$ and $I_c = C\mathrm{d}V_0/\mathrm{d}t$. The free energy of ATP hydrolysis (ΔG_{ATP}) becomes a function of $\ln\{[PCr]/(Total\text{-}Cr - [PCr])^2\}$ (see [18] for details). To a good approximation, $\ln\{[PCr]/(Total\text{-}Cr - [PCr])^2\}$ is linear for PCr between 20% and 70% of total-Cr. The cellular mechanism for mitochondrial respiration and oxygen delivery is illustrated in Fig. 5.2. We have confirmed that both the kinetic and thermodynamic control models of mitochondrial respiration are operative in working human muscles [19].

5.3 Principles of Muscle NIRS

Light within the NIR region (700–3,000 nm) shows less scattering and thus better penetration into biological tissue than visible light. However, light absorption by water limits tissue penetration at longer wavelengths (above ~900 nm), leaving the 700–900 nm window for biological monitoring.

The major absorbing compounds in this wavelength region are vascular hemoglobin (Hb), intracellular Mb, and mitochondrial cytochrome c oxidase [10]. Therefore, NIRS measurements rely on O_2-dependent absorption changes that occur in the heme-containing compounds.

The most common commercially available NIRS devices use single-distance continuous-wave light (NIR_{SDCWS}). To calculate changes in oxy-Hb/Mb, deoxy-Hb/Mb, or total-Hb/Mb, the equation of a two- or multiple-wavelength (770–850 nm) method can be applied according to the following Beer-Lambert Law:

$$\Delta OD = -\log_e(I/I_0) = \varepsilon PL\,\Delta[C], \tag{5.3}$$

$$\Delta[C] = \Delta OD/\varepsilon PL, \tag{5.4}$$

where ε is the extinction coefficient (OD/cm/mM) (= constant), PL is pathlength, $[C]$ is concentration of absorber (mM), I is detected light intensity, I_0 is incident light intensity, and OD is optical density.

A major limitation of NIR_{SDCWS} is that it provides only relative values of tissue oxygenation. The main reason for this lack of quantification by NIR_{SDCWS} is the unknown path of NIR light through biological tissue. The pathlength of NIR light can be measured using other optical approaches, e.g., time-resolved spectroscopy (NIR_{TRS}) [20–23] and phase-modulation spectroscopy (NIR_{PMS}) [23–25]. These approaches provide experimentally observed values of oxygenated and deoxygenated Hb/Mb and Hb/Mb O_2 saturation (SO_2) in skeletal muscle.

With NIR_{TRS}, light is input to tissues in picosecond pulses, and the temporal point spread function (TPSF) is detected as a function of time with picosecond resolution [20, 26]. When a time-correlated single-photon counting system is employed, the distribution of arrival times of a large number of photons follows the TPSF. In principle, the optical properties of tissue can be determined from the TPSF analogous to electronic engineers determining the equivalent circuit of a black box from its response to a voltage or current impulse [26]. Optical properties such as absorption and scattering coefficients can be determined after having an accurate model for light transport in tissues, and represent averaged values for these parameters that best match the monitored data [26].

In NIR_{PMS} instruments, the light source is intensity modulated at radio frequencies (RFs), and measurement is made not only of detected light intensity, but also of its phase shift and modulation depth. Detection of small changes in phase shift and modulation depth is difficult, so almost all these instruments employ some downconversion scheme to bring the RF signal down to an intermediate frequency or audio frequency. In general, two different setups have been used. First, detector gain is modulated at a reference frequency offset by a few kHz from the light source modulation frequency, resulting in direct demodulation within the detector. Second, the detector signal is fed into a double-balanced mixer together with the reference RF, which requires a simpler scheme and much lower RF powers (~10 mW) than the former [26]. The phase shift for typical tissues at frequencies below 200 MHz is linearly related to average optical pathlength. Knowing phase shift enables direct calculation of changes in oxy- and deoxy-hemoglobin concentrations.

Spatially resolved NIR_{SRCWS} (NIR_{SRCWS}) uses multiple light sources coupled to one detector. In NIR_{SRCWS}, the slope of light attenuation versus distance is measured at a distance from the light input, from which the tissue oxygenation index (TOI) can be calculated using photon diffusion theory. Therefore, NIR_{SRCWS} provides relative changes in Hb/Mb and absolute values of SO_2 [27].

With NIR_{SDCWS} measurements, there is an assumption that pathlength does not show significant change during exercise, recovery, and other intervention periods; otherwise, the values obtained are either underestimated or overestimated, as shown in Eqs. 5.3 and 5.4. However, the pathlength of light might vary due to variations in tissue composition, blood volume, and muscle geometry. During

and after arterial occlusion, changes in pathlength for forearm muscle ranged from −8.3% to −2.1% at 780 nm and from −2.2% to 0.74% at 830 nm [22]. Changes in pathlength were less than 10% during arterial occlusion with maximum voluntary contraction (MVC) [21]. The change in pathlength at 780 and 830 nm during forearm exercise from moderate to high intensity and hyperemic recovery was small (<8%) relative to the resting level [28]. The differential pathlength factor (DPF) in thigh muscle decreased slightly, but significantly, from baseline (DPF at 690 nm = 5.22, at 830 nm = 4.49, on average) to peak cycle exercise (DPF at 690 nm = 4.88; at 830 nm = 4.27 on average) (−6.5% at 690 nm and −4.9% at 830 nm) [29]. For an accurate evaluation of muscle oxygenation during arterial occlusion, exercise, and recovery, changes in pathlength should be extensively examined in a wide range of exercise mode/intensity.

5.4 Quantification of In-Vivo NIRS Measurements

5.4.1 Mb/Hb

A recent study reported that the spectral peak appearing around 760 nm in deoxygenated muscle tissue included both deoxy-Hb and deoxy-Mb signals, and that the peak position shifted as a linear function of the relative contributions of Hb and Mb to the optical spectra. The investigators reported that Hb accounts for 87% of the overall signal in mouse muscle but for only 20% in human skeletal muscle [30]. ^{1}H-magnetic resonance spectroscopy (^{1}H-MRS) has also been employed to detect the deoxy-Mb signal by measuring the N-delta proton of proximal histidine [31, 32]. Simulation results based on combined measurements of ^{1}H-MRS and NIRS concluded that the overall NIR signal is greater than ~50% Hb [33]. There is also a report indicating differential kinetics between MbO_2 and NIRS measurements. Another study [34] found that, at rest, human tibialis anterior intramuscular O_2 stores (measured by appearance of ^{1}H-NMR deoxy-Mb signal during cuff occlusion) began to decrease after 1 min and that maximal Mb desaturation was achieved at about 6.5 min. Richardson et al. found that deoxy-Mb levels did not appear to increase after 2 min of cuff ischemia [35], while NIRS-measured oxygen signals declined almost immediately and reached near-maximal levels at 4 min [19]. In contrast, It is reported that deoxy-Mb signal correlated with NIR deoxygenation in a study using ^{1}H-MRS and NIRS [36]. These differing conclusions highlight the need for additional study to clarify not only the contribution of Mb to the NIR signal, but also the kinetics and amount of Mb desaturation during exercise under different conditions.

5.4.2 Effect of Multiple Layers

The light path from a light source to the detector follows a banana-shaped curve in which penetration depth into tissue is approximately equal to half the distance between the light source and detector [12]. If light source–detector separation was set at 3 cm, penetration depth was equal to 1–2 cm and measured volume ~4 cm [12, 37]. Hampson et al. studied how the signal from skin might interfere with muscle NIRS measurement, employing NIR_{SDCWS}, changes in skeletal muscle O_2 content kinetics and skin deoxygenation during 10-min ischemia in human forearm [13]. They found that muscle O_2 content began to fall at onset of arterial occlusion. Increased pressure caused skin oxygenation to rapidly fall within 2–3 min, while muscle oxygenation declined within 6 min. Muscle O_2 content was completely depleted (functional anoxia) about 6 min after onset of arterial occlusion. This indicated that the time course of skin deoxygenation changes during ischemia correlate poorly with changes in skeletal muscle. Heating of the thigh at 37°C and 42°C caused a marked increase in

cutaneous vascular conductance (CVC) at rest and with exercise, and an increase in SO_2 by several percentage points at rest, but not during exercise. One might thus suppose that skin vasodilatation has a marginal influence on NIRS experiments where skin blood flow can change markedly [38]. A fixed source–detector spacing of 4 or 5 cm ensures more accurate quantitation of the oxygenation changes occurring at the muscular level and minimizes the influence of skin vasculature [39].

Subcutaneous adipose tissue thickness has a substantial influence on signal intensity [40–42]: signal intensity for 5-mm fat thickness mm was reduced by ~0.2 (80% of signal for 0 mm) with a source–detector separation of 30–40 mm, and was further reduced by 0.3–0.6 with a separation of 15–20 mm [41, 43]. Other work documented the influence of adipose tissue thickness ranging from 0 to 15 mm with a source–detector separation of 15–40 mm. The curve was based on the results of Monte Carlo simulation as well as in-vivo experiments [41, 43]:

$$S = \exp\left(-(h/A_1)^2\right) - A_2 G(\alpha, \beta), \tag{5.5}$$

where S is normalized measurement sensitivity, h is adipose tissue thickness, $G(\alpha,\beta)$ is a gamma distribution, and constants A_1, A_2, α, and β at a source–detector separation of 15 mm are 6.9, 1.15, 7.86, and 0.80, respectively. Considering that the value of S is mainly determined by h, then corrected values are obtained by dividing the measured values by S.

The influence of adipose tissue thickness in human muscle on NIR spectra was also studied by Monte Carlo simulation in a two-layer model using phantom experiments [44]. The results of this work suggested that subject-to-subject variation in adipose tissue optical coefficients and thickness can be ignored if the thickness is less than 5 mm when the source–detector separation is 40 mm. Subcutaneous adipose tissue thickness should thus be measured for muscle NIRS measurement. In addition, it is preferable to use a 4- to 5-cm source–detector separation for measurements at the muscle level without attenuating signal intensity.

5.5 In-Vitro and In-Vivo Calibration of NIRS Measurements

Several researchers have demonstrated and justified their equations by in-vitro and in-vivo experiments. Chance et al. [12] adopted an "in vitro yeast and blood model" for evaluation of an NIR apparatus. Their model system included intralipid as a scatterer (0.5–1.0%) and blood at concentrations of 10–200 μM hemoglobin. O_2 bubbling caused reoxygenation, while cessation of bubbling caused deoxygenation of hemoglobin due to yeast respiration. Addition of blood correlated with increased in-vivo blood volume. Subtracted signals at 760 and 850 nm showed a linear relationship with hemoglobin deoxygenation [12]. Wilson et al. [45] demonstrated a linear relationship between near-infrared spectroscopic measurements and venous hemoglobin saturation in an animal model. It should be noted that the contribution of Hb/Mb should be different for human and mouse muscle [30]. Mancini et al. found muscle oxygenation and venous O_2 saturation (SvO_2) of human forearm muscles to be closely related during exercise [46]. They also demonstrated that muscle oxygenation decreased with intravascular norepinephrine administration and increased with administration of a vasodilator (nitroprusside). A good association was found between regional quadriceps oxygenation at three different measurement sites and SvO_2 during one-legged dynamic knee extension exercise under normoxic conditions [47]. A good relationship was also found between vastus lateralis oxygenation and femoral arteriovenous O_2 difference (a-vO_2D) during one-legged dynamic knee extension exercise under normoxic as well as hypoxic and hyperoxic conditions [4]. However, several studies have failed to validate NIRS measurement under normoxic conditions

[48, 49]. A possible explanation for this discrepancy is that the NIRS signal contains information on arteriolar, capillary, venular, and intracellular Mb, while the O_2 gradient from arteriole to venule is great during normoxic conditions, such that variations in blood volume from arteriole to venule could alter the NIRS signal without changing venous oxygen signals [40]. Lower oxygen levels during hypoxic conditions would reduce this effect. It is thus broadly accepted that the NIRS oxygenation/deoxygenation signal correlates strongly with changes in SvO_2 and/or a-vO_2D under varying oxygenation status in human muscle.

The use of a physiological calibration in combination with MRS measurements has allowed NIRS to measure muscle oxygen consumption (mVO_2) [19]. The rate of decline of muscle oxygenation during ischemia can be compared with that of muscle PCr in mM/s or a conversion to mVO_2 in mM/s. The transient arterial occlusion method has been used to measure forearm muscle metabolism during exercise [19, 42, 50]. Steady-state exercise at varying intensities was used to provide a range of mVO_2, and resulting mVO_2 values were compared to simultaneous MRS measurements of phosphorus metabolites. A significant correlation was found between mVO_2 and PCr, and ADP concentrations. The linear relationships between exercise intensity and NIRS- and MRS-measured indicators support both thermodynamic [18] and kinetic [15] regulation models of mitochondrial respiration in skeletal muscle. The rate of deoxygenation using transient arterial occlusion has been compared to rate of PCr recovery, a biochemical process of ATP resynthesis via oxidative phosphorylation after exercise (Fig. 5.3). The rate of deoxygenation was quantitatively correlated with the rate of PCr recovery, proving the validity of transient arterial occlusion [50].

Previous studies demonstrated that oxygenation of forearm flexor muscles closely reflects exercise intensity and metabolic rate determined by MRS during exercise and recovery [28, 51], and that muscle oxygenation level (% of arterial occlusion) shows a linear relationship with mVO_2, though in a limited range ($3.2 < mVO_2 <$ 13.3-fold of resting), during exercise and recovery [52]. Therefore, where the transient arterial occlusion method is not applicable, muscle oxygenation level can serve to approximate mVO_2.

5.6 Application of NIRS to Physiological Science

Early studies employed onset and recovery kinetics of oxygen saturation to evaluate oxygen use and oxygen delivery [12]. Muscle reoxygenation recovery time reflects the balance of oxygen delivery and oxygen demand in localized muscles. Recovery time measurements are based on extensive study of PCr recovery time, or on the PCr/Pi ratio. Chance et al. [12] compared male elite rowers to female elite rowers and made suggestions for improved performance. They reported a prolonged recovery time, which suggested increased energy deficit when exercise intensity increased. They also compared recovery time in submaximal and maximal work with plasma lactate, and demonstrated a significant correlation between blood lactate and muscle reoxygenation recovery time after exercise. Several studies have reported that muscle reoxygenaiton recovery time after submaximal to maximal exercise is one of the indicators for evaluating muscle oxidative capacity [12, 53]. The deoxy-Hb/Mb pattern during ramp cycling exercise has been monitored to distinguish trained cyclists from physically active subjects [54]. One set of authors proposed a method for noninvasively approximating muscle capillary blood flow kinetics using the kinetics of the primary component of pulmonary O_2 uptake and deoxy-Hb/Mb in humans during exercise [55]. Other investigators compared rate of deoxygenation at onset of intermittent aerobic plantar flexion (7 on and 3 s off, repeatedly), where anaerobic glycolysis is negligible, to muscle oxidative enzyme activity [56], and demonstrated a good correlation between rate of deoxygenation and citrate synthase activity. Thus, we can assume that the rate of onset of deoxygenation reflects muscle oxidative capacity. One might consider that rate of mitochondrial

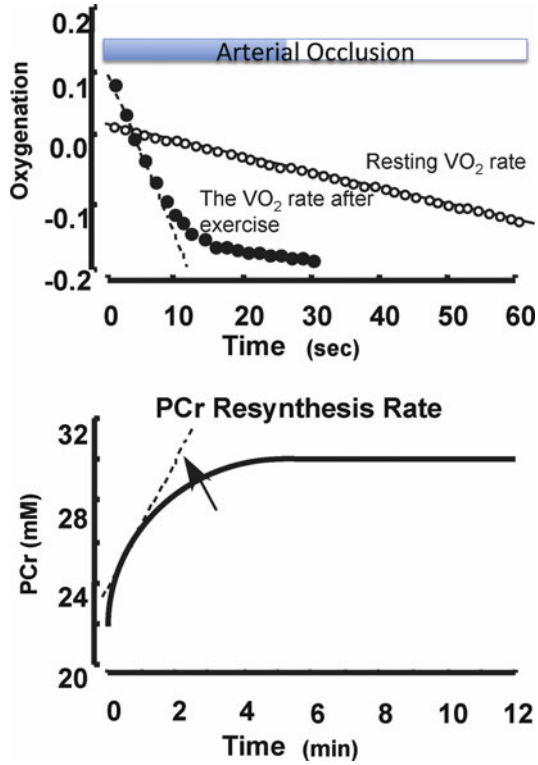

Fig. 5.3 Rate of hemoglobin/myoglobin deoxygenation post-exercise transit ischemia and phosphocreatine (*PCr*) resynthesis rate. Muscle oxygen consumption (VO_2) using the transient arterial occlusion method was compared to rate of PCr recovery, a biochemical process of oxidative ATP resynthesis, at 30 s after exercise. The PCr kinetics is expressed as simulated data (Adapted with permission from J Appl Physiol 90(1):338–344. Copyright © 2001, American Physiological Society)

respiration can be determined by rate of adenine nucleotide translocation and, therefore, that the [ATP]/[ADP] ratio regulates respiratory rate under physiological conditions [16]. However, ATP is maintained constant during submaximal aerobic exercise by creatine kinase equilibrium, so that we need not consider ADP adenine nucleotide translocation during aerobic exercise.

The deoxygenation patterns of the vastus lateralis (VL) and the lateral head of the gastrocnemius (GL) have been examined during graded treadmill exercise [57]. This study found a negative relationship between pulmonary VO_2 and muscle oxygenation level, that the pattern of deoxygenation between VL and GL is somewhat different, and that muscle oxygenation level is associated with pulmonary VO_2. Evaluation of muscle oxygenation in conjunction with systemic oxygen uptake would offer insight into the physiology of healthy and athletic individuals and provide a better exercise prescription for functional improvement. The influence of increased as well as decreased activity on muscle function has also been measured employing NIRS. Most studies have evaluated acute changes in muscle oxygenation during aerobic exercise, but several have also examined high-intensity exercise [58, 59]. In addition, NIRS has been employed to evaluate the training effects of exercise on muscle oxygenation and oxidative metabolism for various types of athletes (e.g., endurance [60, 61] and sprinters [62, 63]) in various sports. Costes et al. [64] attempted to determine whether exercise training–induced adaptations in muscle can be determined by NIRS and found that training does not change the pattern of muscle oxygenation, though a significant

relationship was found between blood lactate and muscle oxygenation at the end of exercise. Motobe et al. [65] used NIRS in immobilized forearm muscle to measure changes in skeletal muscle oxidative function and to evaluate the preventive effect of the endurance training protocol on deterioration of skeletal muscle. They found that muscle oxidative function was determined by the time constant for recovery of mVO_2 applying repeated transient arterial occlusions after exercise (see Fig. 5.4). NIRS measurement indicated delayed mVO_2 recovery after exercise during immobilization.

In summary, NIRS can provide useful information on noninvasive monitoring of deconditioning and reconditioning of skeletal muscle oxidative function. However, most studies on the influence of training have been performed using a cross-sectional study design. There is still a need for more longitudinal studies on exercise training that employ NIRS measurements.

Several multichannel NIRS systems have been developed to detect regional differences in muscle oxygenation [66–68]. By simultaneously collecting data from multiple muscle regions, these devices avoid the variability caused by position-dependent differences in muscle oxygenation that plague all single-location measurements. Imaging devices also allow study of regional differences in how skeletal muscle responds to exercise. Another rationale for using multichannel NIRS systems is that measuring at multiple locations provides better agreement between NIRS signal and oxygen saturation in the entire limb [47]. By simultaneously collecting data from multiple muscle regions, these devices avoid the variability caused by position-dependent differences in muscle oxygenation that plague all single-location measurements. Multichannel NIRS also holds an advantage over NMR and PET devices in terms of better time resolution.

5.7 Application of NIRS to Clinical Practice

The strong dependence of skeletal muscle on oxidative metabolism during exercise means that an improvement in the body's oxidative system leads to higher performance during athletic events. On the other hand, impairment of VO_2 and/or DO_2 will limit performance and thus lead to functional deterioration. NIRS is suitable for measuring attenuation of VO_2 and DO_2 in patients with various diseases and possesses great advantages in terms of portability and real-time monitoring over conventional technologies.

5.7.1 Congestive Heart Failure (CHF)

NIRS has also been employed to evaluate skeletal muscle oxygenation in patients with heart disease. Patients with congestive heart failure (CHF) [45, 69–71] showed greater deoxygenation compared with controls partly due to heart pump failure and the consequent skeletal muscle hypoperfusion. The authors of [71] found a correlation between changes in total hemoglobin (tHb) and leg vessel conductance in patients with and without cardiac dysfunction during submaximal dynamic exercise. This result indicated that tHb reflects muscle vasodilation in these patients and that tHb can be used to assess vascular conductance in this patient group. Another study [72] demonstrated that changes in deoxygenation during submaximal exercise are steeper but peak deoxygenation lower in heart transplant recipients (HTRs) than in control subjects. The authors suggested that NIRS allows for detection of impairment of both DO_2 and O_2 extraction in HTR skeletal muscle. NIRS has also been used to examine the effect of pharmacological treatment on blunted microvascular oxygen delivery to muscle [73] and the effect of rehabilitation on muscle oxygenation [74] in patients with CHF.

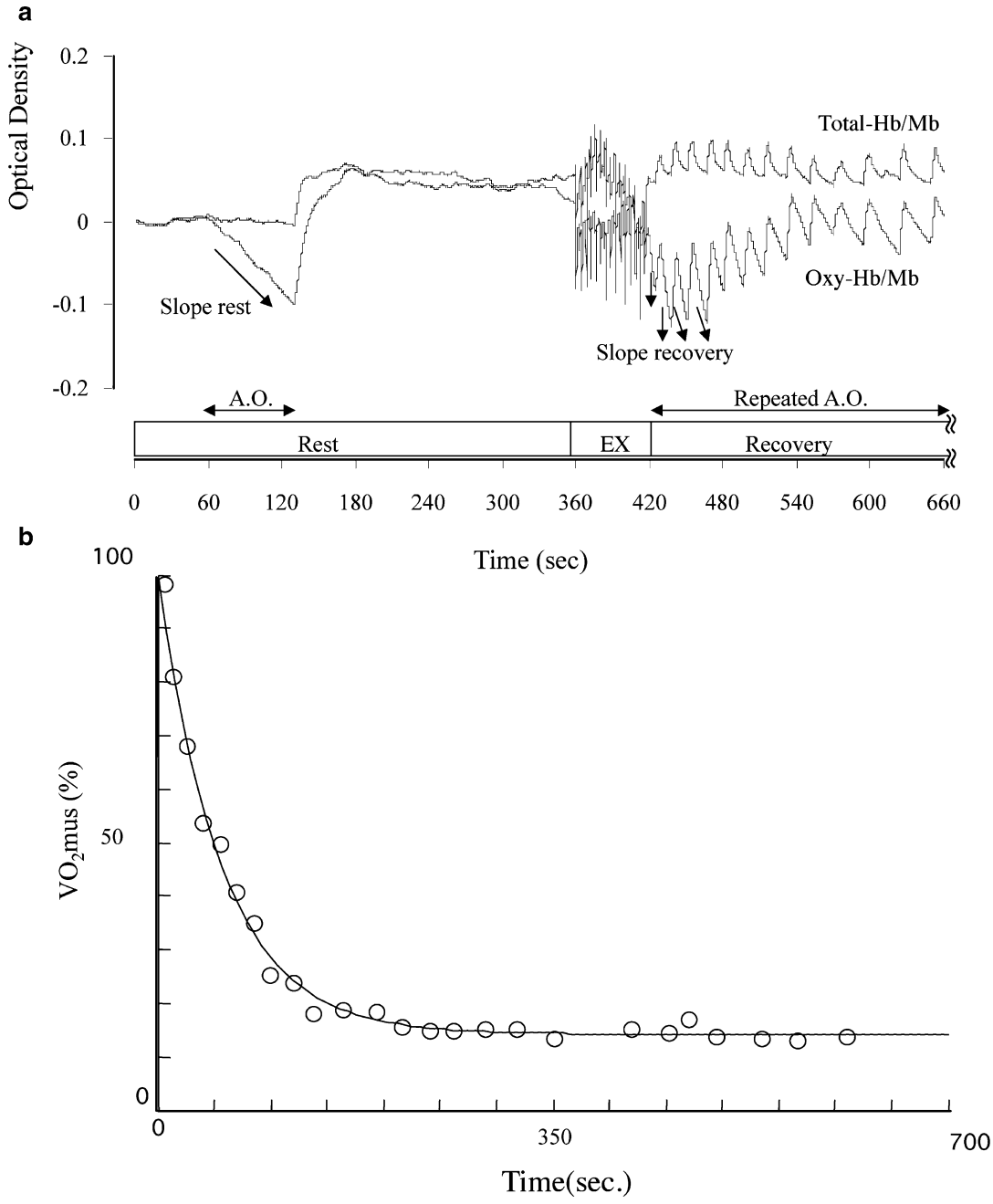

Fig. 5.4 (**a**) **Schematic representation of muscle oxygen consumption (VO_{2mus}mus) and typical changes in muscle oxygenated Hb/Mb**. Schematic representation of VO_2mus and typical changes in muscle oxygenated Hb/Mb at rest and during exercise and recovery. VO_2mus was calculated from the rate of decline of oxygenated Hb/Mb during arterial occlusion (A.O.) at rest (Slope rest), and recovery (Slope recovery). (**b**) **Typical kinetics of VO_2mus recovery after exercise**. VO_2mus during recovery was compared with that at rest, normalized by the maximum value, and plotted as a function of time in seconds. Time constant of VO_2mus for this subject was 56 s (Adapted with permission from Dyn Med 3 Galadriel 3:2. Copyright 2004, BioMed Central)

5.7.2 Patients with Chronic Obstructive Pulmonary Disease (COPD)

Patients with COPD frequently develop skeletal muscle and vascular abnormalities as complications of their disease, similar to those with heart disease [75, 76]. Muscle reoxygenation recovery after exercise has been shown to correlate with pulmonary VO_2 recovery kinetics in patients with COPD [77]. NIRS has also been employed to obtain the time constant of reoxygenation recovery during three work exercise tests, one below and two above the lactic acidosis threshold [78], where patients trained for 6 weeks on a cycle ergometer at high work rates. These investigators found significant correlations between changes in oxidative enzyme activity and changes in recovery time constant and endurance. Leg training is known to accelerate speed of reoxygenation of the vastus lateralis muscle after exercise, and this improvement has been correlated with changes in oxidative enzymes [79].

5.7.3 Neuromuscular Disorders

NIRS has also been employed to study patients with neuromuscular disorders. An increase in muscle oxygenation (paradoxical oxygenation) at onset of treadmill exercise was been reported in patients with cytochrome c oxidase deficiency [80], metabolic myopathy [81], and Friedreich's ataxia [82]. This paradoxical oxygenation, a diagnostic indicator, is due to a combination of impaired mVO_2 and a normal physiological increase of DO_2 (vasodilatation) stimulated by muscle pump and/or myogenic activity. Grassi et al. [83] tested patients with mitochondrial myopathy (MM) or myophosphorylase deficiency (McArdle's disease, McA) for changes in capacity for O_2 extraction, maximal aerobic power, and exercise tolerance during cycle exercise using NIRS. They found that peak deoxygenation during exercise, an index of O_2 extraction, was lower in MM and McA than in controls.

5.7.4 Peripheral Arterial Disease (PAD)

Several studies have used rate of recovery of reoxygenation to evaluate DO_2 in the calf muscles of patients with peripheral artery disease (PAD) [84]. In a rather extensive study, the authors of [85] reported good agreement between faster PCr recovery kinetics and better oxygenation kinetics measured by NIRS [85]. A slower rate of calf reoxygenation after exercise is a consistent finding in PAD patients (see [86–88]).

Patients with varying severity of PAD have been classified by using patterns of calf oxygenation kinetics during treadmill exercise and recovery [87]. Impaired muscle O_2 usage at rest [89] and at onset of exercise [90] have been observed as well. The authors of [84] found a good correlation between Doppler pressure waveform measurements and ankle arm systolic pressures (AAI) and the NIRS recovery time constant [84]. Mohler et al. [86] examined the interaction between PAD and presence or absence of diabetes mellitus (DM) employing changes in muscle capillary blood expansion and reoxygenation recovery, and found that capillary blood expansion is reduced in patients with DM regardless of existence of PAD. This parameter might thus be a good indicator of vascular impairment in patients with DM. Peripheral venous occlusive disease (PVOD) has also been tested using NIRS [91–93], and investigators were able to distinguish between successfully treated patients and those with deep vein thrombosis after 12 months. So we can conclude that NIRS is able to identify and quantify severity of DO_2 in patients with PAD and PVOD.

5.7.5 Spinal Cord Injury (SCI)

NIRS has also been employed to evaluate changes in oxygenation that occur in the leg muscles of patients with spinal cord injury (SCI). Bhambhani et al. [94] found lower muscle deoxygenation during maximal exercise and faster changes in muscle deoxygenation with respect to pVO_2 during functional electrical stimulation cycle exercise in SCI patients compared to healthy subjects. NIRS has been used to evaluate potential SCI therapies. The authors of [95] placed motor-complete SCI subjects and neurologically normal controls on a gait-training apparatus that enabled subjects to stand and move their legs passively, and found that oxygenation gradually increased and deoxygenation decreased in the experimental group, quite different from the response in normal controls. This result demonstrated that passive leg movement can not only induce muscular activity but can also alter muscle oxygenation in a paralyzed lower leg, and that induced muscular activity seems to correlate with increased muscle perfusion. In another NIRS study [96], SCI patients underwent electrical stimulation training (45 min daily, 3 days a week for 10 weeks) with different muscle oxygenation loads in paralyzed lower limbs. The vastus lateralis muscle of statically trained legs was found to show significantly increased oxidative capacity compared to both baseline and dynamically trained legs. This study demonstrated that NIRS is able to detect attenuated muscle deoxygenation after static training.

5.7.6 End-Stage Renal Disease (ESRD)

Muscle oxygenation and metabolism were examined using NIRS in children with end-stage renal disease (ESRD) before and after kidney transplantation and compared to controls during submaximal handgrip exercise [97]. These investigators looked at rate of deoxygenation, an indicator of mVO_2, during transient arterial occlusion post-exercise and recovery time to reoxygenation after exercise. Both parameters were significantly improved after renal transplantation but not significantly different from controls (Fig. 5.5). Another group [98] employed NIRS to evaluate the potential for vascular and metabolic dysfunction in patients with renal failure, the effect of handgrip exercise training on forearm vasodilator responses, and forearm vasodilator responses to 3-min arterial occlusion in patients receiving hemodialysis, but found no improvement in vasodilator response after exercise training, and vasodilator response estimated by maximum oxygenation after release of arterial occlusion was significantly smaller in renal failure patients compared to controls. These studies show that NIRS can be used to detect muscle hypoperfusion in patients with renal failure and to find the functional alterations of muscle oxidative metabolism that occur after renal transplantation.

The results of clinical NIRS application suggest that it is a promising tool for noninvasively monitoring metabolic impairment in a follow-up setting, and in assessment of therapies and interventions.

5.8 Summary

There are several issues involved with in-vivo muscle NIRS measurement: (a) the origin of the NIR signal (from arterioles, capillary, and venules, as well as from Hb and Mb); (b) the NIR penetration depth or measurement area in tissue with varying source–detector arrangements in a multilayer model, including the effect of non-muscular tissue; (c) changes in optical properties within a wide

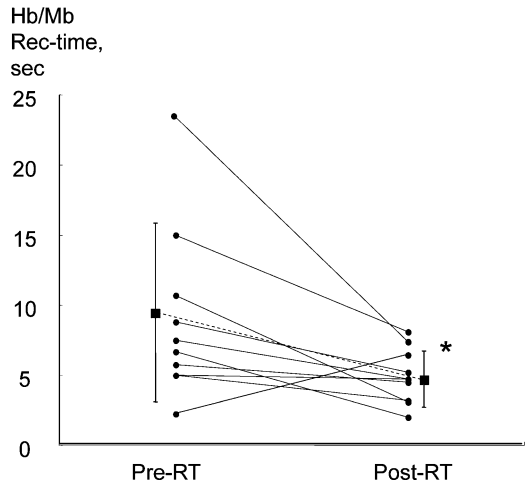

Fig. 5.5 Changes in recovery time (Rec-time) for Hb/Mb reoxygenation after renal transplantation (RT) in 10 renal transplant recipients. Individual data shown in *black circles* and *solid lines*; mean and SD shown in *black squares* and *dotted line*. Significant difference $p < 0.05$. Recovery time after transplantation was shortened in nine patients and delayed in one patient, who showed the shortest TR before RT (Adapted with permission from Am J Kidney Dis 48:473–480. Copyright © 2006, Elsevier)

range of tissue oxygenation status; (d) the wide variety of subjects; and (e) the choice of exercise modality. Nevertheless, there is little question that NIRS is suitable and quite useful for measuring changes in mVO_2 and DO_2 in healthy subjects as well as in patients with various disease states (e.g., chronic heart failure, chronic obstructive pulmonary disease, various muscle diseases, peripheral vascular disease, spinal cord injury, renal failure). In addition, NIRS has great advantages over conventional technologies in terms of portability and real-time monitoring.

Acknowledgments I would like to acknowledge funding support from the Ministry of Education, Culture, Sports, Science, and Technology of Japan.

Problems

5.1 How would you quantify muscle NIR signals?

5.2 List the various muscle NIR indicators. Which indicator reflects muscle oxidative function? How?

Further Reading

Ferrari M, Muthalib M, Quaresima V (2011) The use of near-infrared spectroscopy in understanding skeletal muscle physiology: recent developments. Philos Trans A Math Phys Eng Sci 369:4577–4590.

Hamaoka T, McCully K, Quaresima V, Yamamoto K, Chance B (2007) Near-infrared spectroscopy/imaging for monitoring muscle oxygenation and oxidative metabolism in healthy and diseased humans. J Biomed Opt 12(6):62105–62120.

Hamaoka T, McCully K, Quaresima V, Yamamoto K, Chance B (2011) The use of muscle near-infrared spectroscopy in sport, health, and medical sciences: recent developments. Philos Trans A Math Phys Eng Sci 369:4591–4604.
Yamamoto K, Niwayama M, Lin L, Shiga T, Kudo N, Takahashi M (1998) Accurate NIRS measurement of muscle oxygenation by correcting the influence of a subcutaneous fat layer. Proc SPIE 3194:166–173.

References

1. Welch HG, Bonde-Petersen F, Graham T, Klausen K, Secher N (1977) Effects of hyperoxia on leg blood flow and metabolism during exercise. J Appl Physiol 42:385–390
2. Gayeski TE, Honig CR (1983) Direct measurement of intracellular O_2 gradients; role of convection and myoglobin. Adv Exp Med Biol 159:613–621
3. Bhambhani YN (2004) Muscle oxygenation trends during dynamic exercise measured by near infrared spectroscopy. Can J Appl Physiol 29:504–523
4. Boushel B, Langberg H, Olesen J, Gonzales-Alonzo J, Bulow J, Kjaer M (2001) Monitoring tissue oxygen availability with near infrared spectroscopy (NIRS) in health and disease. Scand J Med Sci Sports 11:213–222
5. Ferrari M, Mottola L, Quaresima V (2004) Principles, techniques, and limitations of near infrared spectroscopy. Can J Appl Physiol 29:463–487
6. Hamaoka T, McCully K, Quaresima V, Yamamoto K, Chance B (2007) Near-infrared spectroscopy/imaging for monitoring muscle oxygenation and oxidative metabolism in healthy and diseased humans. J Biomed Opt 12(6):62105–62120
7. Millikan GA (1933) A simple photoelectric colorimeter. J Physiol 79:152–157
8. Chance B (1954) Spectrophotometry of intracellular respiratory pigments. Science 120:767–775
9. Chance B, Connelly CM (1957) A method for the estimation of the increase in concentration of adenosine diphosphate in muscle sarcosomes following a contraction. Nature 179:1235–1237
10. Jöbsis FF (1977) Noninvasive, infrared monitoring of cerebral and myocardial oxygen sufficiency and circulatory parameters. Science 198:1264–1267
11. McCully KK, Kakihira H, Vandenborne K, Kent-Braun J (1991) Noninvasive measurements of activity-induced changes in muscle metabolism. J Biomech 24:153–161
12. Chance B, Dait MT, Zhang C, Hamaoka T, Hagerman F (1992) Recovery from exercise-induced desaturation in the quadriceps muscles of elite competitive rowers. Am J Physiol 262:C766–C775
13. Hampson NB, Piantadosi CA (1988) Near infrared monitoring of human skeletal muscle oxygenation during forearm ischemia. J Appl Physiol 64(6):2449–2457
14. Chance B, Williams GR (1955) Respiratory enzymes in oxidative phosphorylation, I: kinetics of oxygen utilization. J Biol Chem 217:409–427
15. Chance B, Leigh JS, Kent-Braun JA, McCully K, Nioka S, Clark BJ, Maris JM, Graham T (1986) Multiple controls of oxidative metabolism in living tissues as studied by phosphorus magnetic resonance. Proc Natl Acad Sci USA 83:9458–9462
16. Klingenberg M (1980) The ADP–ATP translocation in mitochondria, a membrane potential controlled transport. J Membr Biol 56(2):97–105
17. Holian A, Owen CS, Wilson DF (1977) Control of respiration in isolated mitochondria: quantitative evaluation of the dependence of respiratory rates on [ATP], [ADP], and [Pi]. Arch Biochem Biophys 181:164–171
18. Meyer RA (1988) A linear model of muscle respiration explains monoexponential phosphocreatine changes. Am J Physiol 254:C548–C553
19. Hamaoka T, Iwane H, Shimomitsu T, Katsumura T, Murase N, Nishio S, Osada T, Kurosawa Y, Chance B (1996) Noninvasive measures of oxidative metabolism on working human muscles by near-infrared spectroscopy. J Appl Physiol 81:1410–1417
20. Chance B, Nioka S, Kent-Braun J, McCully K, Fountain M, Greenfeld R, Holtom G (1988) Time-resolved spectroscopy of hemoglobin and myoglobin in resting and ischemic muscle. Anal Biochem 174:698–707
21. Ferrari M, Wei Q, Carraresi L, De Blasi RA, Zaccanti G (1992) Time-resolved spectroscopy of the human forearm. J Photochem Photobiol B 16:141–153
22. Hamaoka T, Katsumura T, Murase N, Nishio S, Osada T, Sako T, Higuchi H, Kurosawa Y, Shimomitsu T, Miwa M, Chance B (2000) Quantification of ischemic muscle deoxygenation by near infrared time-resolved spectroscopy. J Biomed Opt 5:102–105
23. Delpy DT, Cope M, van der Zee P, Arridge S, Wray S, Wyatt J (1988) Estimation of optical pathlength through tissue from direct time of flight measurement. Phys Med Biol 33:1433–1442
24. Wolf M, Wolf U, Choi JH, Gupta R, Safonova LP, Paunescu LA, Michalos A, Gratton E (2002) Functional frequency-domain near-infrared spectroscopy detects fast neuronal signal in the motor cortex. Neuroimage 17:1868–1875

25. Duncan A, Meek JH, Clemence M, Elwell CE, Tyszczuk L, Cope M, Delpy DT (1995) Optical pathlength measurements on adult head, calf and forearm and the head of the newborn infant using phase resolved optical spectroscopy. Phys Med Biol 40:295–304
26. Delpy DT, Cope M (1997) Quantification in tissue near-infrared spectroscopy. Philos Trans Roy Soc Lond B 352:649–659
27. Quaresima V, Homma S, Azuma K, Shimizu S, Chiarotti F, Ferrari M, Kagaya A (2001) Calf and shin muscle oxygenation patterns and femoral artery blood flow during dynamic plantar flexion exercise in humans. Eur J Appl Physiol Occup Physiol 84:387–394
28. Hamaoka T, Osada T, Murase N, Sako T, Higuchi H, Kurosawa Y, Miwa M, Katsumura T, Chance B (2003) Quantitative evaluation of oxygenation and metabolism in the human skeletal muscle. Opt Rev 10(5):493–497
29. Ferreira LF, Hueber DM, Barstow TJ (2007) Effects of assuming constant optical scattering on measurements of muscle oxygenation by near-infrared spectroscopy during exercise. J Appl Physiol 102:358–367
30. Marcinek DJ, Amara CE, Matz K, Conley KE, Schenkman KA (2007) Wavelength shift analysis: a simple method to determine the contribution of hemoglobin and myoglobin to in vivo optical spectra. Appl Spectrosc 61(6):665–669
31. Wang ZY, Noyszewski EA, Leigh JS Jr (1990) In vivo MRS measurement of deoxymyoglobin in human forearms. Magn Reson Med 14:562–567
32. Mole PA, Chung Y, Tran TK, Sailasuta N, Hurd R, Jue T (1999) Myoglobin desaturation with exercise intensity in human gastrocnemius muscle. Am J Physiol 277:R173–R180
33. Nioka S, Wang DJ, Im J, Hamaoka T, Wang ZJ, Leigh JS, Chance B (2006) Simulation of Mb/Hb in NIRS and oxygen gradient in the human and canine skeletal muscles using H-NMR and NIRS. Adv Exp Med Biol 578:223–228
34. Lanza IR, Tevald MA, Befroy DE, Kent-Braun JA (2010) Intracellular energetics and critical PO_2 in resting ischemic human skeletal muscle in vivo. Am J Physiol Regul Integr Comp Physiol 299:R1415–R1422
35. Richardson RS, Newcomer SC, Noyszewski EA (2001) Skeletal muscle intracellular PO_2 assessed by myoglobin desaturation: response to graded exercise. J Appl Physiol 91:2679–2685
36. Tran TK, Sailasuta N, Kreutzer U, Hurd R, Chung Y, Mole P, Kuno S, Jue T (1999) Comparative analysis of NMR and NIRS measurements of intracellular PO_2 in human skeletal muscle. Am J Physiol 276:R1682–R1690
37. Chance B, Nioka S, Kent J, McCully K, Fountain M, Greenfeld R, Holtom G (1988) Time-resolved spectroscopy of hemoglobin and myoglobin in resting and ischemic muscle. Anal Biochem 174:698–707
38. Tew GA, Ruddock AD, Saxton JM (2010) Skin blood flow differentially affects near-infrared spectroscopy-derived measures of muscle oxygen saturation and blood volume at rest and during dynamic leg exercise. Eur J Appl Physiol 110(5):1083–1089
39. Ferrari M, Cettolo V, Quaresima V (2006) Light source-detector spacing of near-infrared-based tissue oximeters and the influence of skin blood flow. J Appl Physiol 100(4):1426–1427
40. McCully KK, Hamaoka T (1998) Near-infrared spectroscopy: what can it tell us about oxygen saturation in skeletal muscle? Exerc Sport Sci Rev 28:123–127
41. Yamamoto K, Niwayama M, Lin L, Shiga T, Kudo N, Takahashi M (1998) Accurate NIRS measurement of muscle oxygenation by correcting the influence of a subcutaneous fat layer. Proc SPIE 3194:166–173
42. Van Beekvelt MC, Borghuis MS, Van Engelen BG, Wevers RA, Colier WN (2001) Adipose tissue thickness affects in vivo quantitative near-IR spectroscopy in human skeletal muscle. Clin Sci (Lond) 101:21–28
43. Niwayama M, Yamamoto K, Kohata D, Hirai K, Kudo N, Hamaoka T, Kime R, Katsumura T (2002) A 200-channel imaging system of muscle oxygenation using CW near-infrared spectroscopy. IEICE Trans Inf Syst E85-D(1): 115–123
44. Yang Y, Soyemi OO, Landry MR, Soller BR (2005) Influence of a fat layer on the near infrared spectra of human muscle: quantitative analysis based on two-layered Monte Carlo simulations and phantom experiments. Opt Express 13:1570–1579
45. Wilson JR, Mancini DM, McCully K, Ferraro N, Lanoce V, Chance B (1989) Noninvasive detection of skeletal muscle underperfusion with near-infrared spectroscopy in patients with heart failure. Circulation 80:1668–1674
46. Mancini DM, Bolinger L, Li H, Kendrick K, Chance B, Wilson JR (1994) Validation of near-infrared spectroscopy in humans. J Appl Physiol 77:2740–2747
47. Esaki K, Hamaoka T, Radegran G, Boushel R, Hansen J, Katsumura T, Haga S, Mizuno M (2005) Association between regional quadriceps oxygenation and blood oxygen saturation during normoxic one-legged dynamic knee extension. Eur J Appl Physiol Occup Physiol 95:361–370
48. Costes F, Barthelemy JC, Feasson L, Busso T, Geyssant A, Denis C (1996) Comparison of muscle near-infrared spectroscopy and femoral blood gases during steady-state exercise in humans. J Appl Physiol 80:1345–1350
49. MacDonald MJ, Tarnopolsky MA, Green HJ, Hughson RL (1999) Comparison of femoral blood gases and muscle near-infrared spectroscopy at exercise onset in humans. J Appl Physiol 86:687–693

50. Sako T, Hamaoka T, Higuchi H, Kurosawa Y, Katsumura T (2001) Validity of NIR spectroscopy for quantitatively measuring muscle oxidative metabolic rate in exercise. J Appl Physiol 90(1):338–344
51. Boushel R, Pott F, Madsen P, Radegran G, Nowak M, Quistorff B, Secher N (1998) Muscle metabolism from near infrared spectroscopy during rhythmic handgrip in humans. Eur J Appl Physiol Occup Physiol 79:41–48
52. Homma T, Hamaoka T, Sako T, Murakami M, Esaki K, Kime R, Ueda C, Nagasawa T, Katsumura T (2005) Muscle oxidative metabolism accelerates with mild acidosis during incremental intermittent isometric plantar flexion exercise. Dyn Med 4:2
53. Ichimura S, Murase N, Osada T, Kime R, Homma T, Ueda C, Nagasawa T, Motobe M, Hamaoka T, Katsumura T (2006) Age and activity status affect muscle reoxygenation time after maximal cycling exercise. Med Sci Sports Exerc 38:1277–1281
54. Boone J, Koppo K, Barstow TJ, Bouckaert J (2009) Pattern of deoxy[Hb + Mb] during ramp cycle exercise: influence of aerobic fitness status. Eur J Appl Physiol 105(6):851–859
55. Ferreira LF, Townsend DK, Lutjemeier BJ, Barstow TJ (2005) Muscle capillary blood flow kinetics estimated from pulmonary O_2 uptake and near-infrared spectroscopy. J Appl Physiol 98(5):1820–1828
56. Hamaoka T, Mizuno M, Katsumura T, Osada T, Shimomitsu T, Quistorff B (1998) Correlation between indicators determined by near infrared spectroscopy and muscle fiber types in humans. Jpn J Appl Physiol 28(5):339–344
57. Hiroyuki H, Hamaoka T, Sako T, Nishio S, Kime R, Murakami M, Katsumura T (2002) Oxygenation in vastus lateralis and lateral head of gastrocnemius during treadmill walking and running in humans. Eur J Appl Physiol 87:343–349
58. Bae S, Hamaoka T, Katsumura T, Shiga T, Ohno H, Haga S (2000) Comparison of muscle oxygen consumption measured by near infrared continuous wave spectros copy during supramaximal and intermittent pedalling exercise. Int J Sports Med 21:168–174
59. Bhambhani Y, Maikala R, Esmail S (2001) Oxygenation trends in vastus lateralis muscle during incremental and intense anaerobic cycle exercise in young men and women. Eur J Appl Physiol 84:547–556
60. Neary JP (2004) Application of near infrared spectroscopy to exercise sports science. Can J Appl Physiol 29:488–503
61. Legrand R, Ahmaidi S, Moalla W, Chocquet D, Marles A, Prieur F, Mucci P (2005) O_2 arterial desaturation in endurance athletes increases muscle deoxygenation. Med Sci Sports Exerc 37:782–788
62. Ding H, Wang G, Lei W, Wang R, Huang L, Xia Q, Wu J (2001) Non-invasive quantitative assessment of oxidative metabolism in quadriceps muscles by near infrared spectroscopy. Br J Sports Med 35:441–444
63. Hoffman JR, Im J, Rundell KW, Kang J, Nioka S, Spiering BA, Kime R, Chance B (2003) Effect of muscle oxygenation during resistance exercise on anabolic hormone response. Med Sci Sports Exerc 35:1929–1934
64. Costes F, Prieur F, Feasson L, Geyssant A, Barthelemy JC, Denis C (2001) Influence of training on NIRS muscle oxygen saturation during submaximal exercise. Med Sci Sports Exerc 33:1484–1489
65. Motobe M, Murase N, Osada T, Homma T, Ueda C, Nagasawa T, Kitahara A, Ichimura S, Kurosawa Y, Katsumura T, Hoshika A, Hamaoka T (2004) Noninvasive monitoring of deterioration in skeletal muscle function with forearm cast immobilization and the prevention of deterioration. Dyn Med 3:2
66. Kime R, Im J, Moser D, Lin Y, Nioka S, Katsumura T, Chance B (2005) Reduced heterogeneity of muscle deoxygenation during heavy bicycle exercise. Med Sci Sports Exerc 37:412–417
67. Miura H, McCully K, Hong L, Nioka S, Chance B (2001) Regional difference of muscle oxygen saturation and blood volume during exercise determined by near infrared imaging device. Jpn J Physiol 51:599–606
68. Wolf U, Wolf M, Choi JH, Paunescu LA, Safonova LP, Michalos A, Gratton E (2003) Mapping of hemodynamics on the human calf with near infrared spectroscopy and the influence of the adipose tissue thickness. Adv Exp Med Biol 510:225–230
69. Hanada A, Okita K, Yonezawa K, Ohtsubo M, Kohya T, Murakami T, Nishijima H, Tamura M, Kitabatake A (2000) Dissociation between muscle metabolism and oxygen kinetics during recovery from exercise in patients with chronic heart failure. Heart 83:161–166
70. Matsui S, Bolinger L, Li H, Kendrick K, Chance B, Wilson JR (1995) Assessment of working muscle oxygenation in patients with chronic heart failure. Am Heart J 125:690–695
71. Watanabe S, Ishii C, Takeyasu N, Ajisaka R, Nishina H, Morimoto T, Sakamoto K, Eda K, Ishiyama M, Saito T, Aihara H, Arai E, Toyama M, Shintomi Y, Yamaguchi I (2005) Assessing muscle vasodilation using near-infrared spectroscopy in cardiac patients. Circ J 69:802–814
72. Lanfranconi F, Borrelli E, Ferri A, Porcelli S, Maccherini M, Chiavarelli M, Grassi B (2006) Noninvasive evaluation of skeletal muscle oxidative metabolism after heart transplant. Med Sci Sports Exerc 38:1374–1383
73. Sperandio PA, Borghi-Silva A, Barroco A, Neder JA (2009) Microvascular oxygen delivery-to-utilization mismatch at the onset of heavy-intensity exercise in optimally treated patients with CHF. Am J Physiol Heart Circ Physiol 297:H1720–H1728

74. Gerovasili V, Drakos S, Kravari M, Malliaras K, Karatzanos E, Dimopoulos S, Tasoulis A, Anastasiou-Nana M, Roussos C, Nanas S (2009) Physical exercise improves the peripheral microcirculation of patients with chronic heart failure. J Cardiopulm Rehabil Prev 29:385–391
75. Serres I, Hayot M, Prefaut C, Mercier J (1998) Skeletal muscle abnormalities in patients with COPD: contribution to exercise intolerance. Med Sci Sports Exerc 30:1019–1027
76. Maltais F, LeBlanc P, Jobin J, Casaburi R (2000) Peripheral muscle dysfunction in chronic obstructive pulmonary disease. Clin Chest Med 21:665–677
77. Okamoto T, Kanazawa H, Hirata K, Yoshikawa J (2003) Evaluation of oxygen uptake kinetics and oxygen kinetics of peripheral skeletal muscle during recovery from exercise in patients with chronic obstructive pulmonary disease. Clin Physiol Funct Imaging 23:257–262
78. Puente-Maestu L, Tena T, Trascasa C, Perez-Parra J, Godoy R, Garcia MJ, Stringer WW (2003) Training improves muscle oxidative capacity and oxygenation recovery kinetics in patients with chronic obstructive pulmonary disease. Eur J Appl Physiol Occup Physiol 88:580–587
79. Rondelli RR, Dal Corso S, Simões A, Malaguti C (2009) Methods for the assessment of peripheral muscle fatigue and its energy and metabolic determinants in COPD. J Bras Pneumol 35:1125–1135
80. Bank W, Chance B (1994) An oxidative defect in metabolic myopathies: diagnosis by noninvasive tissue oximetry. Ann Neurol 36:830–837
81. Grassi B, Porcelli S, Marzorati M, Lanfranconi F, Vago P, Marconi C, Morandi L (2009) Metabolic myopathies: functional evaluation by analysis of oxygen uptake kinetics. Med Sci Sports Exerc 41:2120–2127
82. Lynch DR, Lech G, Farmer JM, Balcer LJ, Bank W, Chance B, Wilson RB (2002) Near infrared muscle spectroscopy in patients with Friedreich's ataxia. Muscle Nerve 25:664–673
83. Grassi B, Marzorati M, Lanfranconi F, Ferri A, Longaretti M, Stucchi A, Vago P, Marconi C, Morandi L (2007) Impaired oxygen extraction in metabolic myopathies: detection and quantification by near-infrared spectroscopy. Muscle Nerve 35:510–520
84. McCully KK, Halber C, Posner JD (1994) Exercise-induced changes in oxygen saturation in the calf muscles of elderly subjects with peripheral vascular disease. J Gerontol 49:B128–B134
85. McCully KK, Iotti S, Kendrick K, Wang Z, Posner JD, Leigh J Jr, Chance B (1994) Simultaneous in vivo measurements of HbO_2 saturation and PCr kinetics after exercise in normal humans. J Appl Physiol 77:5–10
86. Mohler ER 3rd, Lech G, Supple GE, Wangb H, Chance B (2006) Impaired exercise-induced blood volume in type 2 diabetes with or without peripheral arterial disease measured by continuous-wave near-infrared spectroscopy. Diabetes Care 29:1856–1859
87. Komiyama T, Shigematsu H, Yasuhara H, Hosoi Y, Muto T (1996) An objective evaluation of muscle oxygen content in claudicants receiving drug therapy. Int Angiol 15:215–218
88. Komiyama T, Shigematsu H, Yasuhara H, Muto T (2000) Near-infrared spectroscopy grades the severity of intermittent claudication in diabetics more accurately than ankle pressure measurement. Br J Surg 87:459–466
89. Malagoni AM, Felisatti M, Mandini S, Mascoli F, Manfredini R, Basaglia N, Zamboni P, Manfredini F (2010) Resting muscle oxygen consumption by near-infrared spectroscopy in peripheral arterial disease: a parameter to be considered in a clinical setting? Angiology 61:530–536
90. Bauer TA, Brass EP, Hiatt WR (2004) Impaired muscle oxygen use at onset of exercise in peripheral arterial disease. J Vasc Surg 40:488–493
91. Pedersen BL, Baekgaard N, Quistorff B (2009) Muscle mitochondrial function in patients with type 2 diabetes mellitus and peripheral arterial disease: implications in vascular surgery. Eur J Vasc Endovasc Surg 38:356–364
92. Hosoi Y, Yasuhara H, Shigematsu H, Aramoto H, Komiyama T, Muto T (1997) A new method for the assessment of venous insufficiency in primary varicose veins using near-infrared spectroscopy. J Vasc Surg 26:53–60
93. Yamaki T, Nozaki M, Sakurai H, Takeuchi M, Soejima K, Kono T (2006) The utility of quantitative calf muscle near-infrared spectroscopy in the follow-up of acute deep vein thrombosis. J Thromb Haemost 4:800–806
94. Bhambhani Y, Tuchak C, Burnham R, Jeon J, Maikala R (2000) Quadriceps muscle deoxygenation during functional electrical stimulation in adults with spinal cord injury. Spinal Cord 38:630–638
95. Kawashima N, Nakazawa K, Akai M (2005) Muscle oxygenation of the paralyzed lower limb in spinal cord-injured persons. Med Sci Sports Exerc 37:915–921
96. Crameri RM, Cooper P, Sinclair PJ, Bryant G, Weston A (2004) Effect of load during electrical stimulation training in spinal cord injury. Muscle Nerve 29:104–111
97. Matsumoto N, Ichimura S, Hamaoka T, Osada T, Hattori M, Miyakawa S (2006) Impaired muscle oxygen metabolism in uremic children: improved after renal transplantation. Am J Kidney Dis 48:473–480
98. Kuge N, Suzuki T, Isoyama S (2005) Does handgrip exercise training increase forearm ischemic vasodilator responses in patients receiving hemodialysis? Tohoku J Exp Med 207:303–312